

Geometry and slip rate of the Aigion Fault, a young normal fault system in the western Gulf of Corinth

L.C. McNeill

C.J. Cotterill*

J.M. Bull

T.J. Henstock

R. Bell

National Oceanography Centre, School of Ocean and Earth Science, University of Southampton, Southampton SO14 3ZH, UK

A. Stefatos

Laboratory of Marine Geology and Physical Oceanography, University of Patras, Patras 26500, Greece

*Current address: British Geological Survey, West Mains Road, Edinburgh, EH9 3LA

ABSTRACT

The Aigion fault is one of the youngest major normal faults in the Gulf of Corinth, Greece, with an immature displacement profile. Based on geometry, slip rate and comparison with regional faults, we estimate the fault system length at ~10 km. We find the slip rate of the fault system is $\sim 3.5 \pm 1$ mm/yr decreasing to $\sim 2.5 \pm 0.7$ mm/yr close to its eastern tip. Complex fault geometry and displacement profiles on the shelf east of Aigion are consistent with the latter as the eastern tip location. Analysis of slip on this fault system and the established fault to the south (Western Eliki Fault) suggests that slip was transferred rapidly but not homogeneously between the two faults during the period of contemporaneous activity. Together with a lack of evidence of lateral propagation at the eastern fault tip in the last 10–13 k.y., we suggest that the fault developed and established its current length rapidly, within

its 200–300 k.y. history. These results contribute to our understanding of the process of northward fault migration into the rift and the development of new normal faults.

Keywords: Corinth rift, normal faults, continental rifting, fault development

INTRODUCTION

The Gulf of Corinth is renowned for high extension rates, seismicity and dramatic rift morphology. Our understanding of the rift geometry has evolved over the last decade from a simple half-graben model to a more complex model of varying geometry in space and time, with multiple major faults accommodating strain across the rift and hangingwall migration of rift-bounding faults (e.g., Armijo et al., 1996; Moretti et al., 2003; Stefatos et al., 2002; DeMartini et al., 2004; McNeill et al., 2005).

The Aigion fault system (AF, Fig. 1) in the western Gulf is unusual for two reasons: it is contemporaneously active with part of an overlapping fault system (Western Eliki) and has a non-constant (and limited) displacement profile with decreasing displacement from west to east. It has therefore been interpreted as an immature fault (e.g., DeMartini et al., 2004; Micarelli et al., 2003), probably propagating to the east and possibly part of the northward fault migration in the rift. No historic earthquakes are confirmed on the Aigion fault but paleoseismological studies confirm Holocene activity (Pantosti et al., 2004) potentially supported by microseismicity (e.g., Rigo et al., 1996). Cracks, coastal slumping and liquefaction in the Aigion area resulted from an offshore-generated earthquake in 1995.

We collected high resolution seismic and multibeam bathymetric data in the western Gulf of Corinth in July, 2003 (McNeill et al., 2005; Cotterill, 2006 for further details). A grid of 25–100 m spaced multichannel boomer seismic lines were collected over the shelf east of Aigion (Fig. 1). Using these high resolution data, this paper reveals the geometry of the eastern extension and tip of the Aigion fault system (Offshore Aigion Fault, OAF), and integrates offshore and onshore data to assess geometry and slip rates of the fault system as a

whole. We will analyze the Aigion fault age and evidence for rate of fault development and lateral growth to contribute to ongoing debate. This study will also provide insight into the development of new fault systems in this and other continental rifts.

Seismic Stratigraphy

High resolution seismic data resolve sub-horizontal topsets and dipping foresets of the fan delta which are interpreted to represent ~0-80 ka since the last highstand (Fig. 2) based on comparisons with similar studies (e.g., Leeder et al., 2005). Within these deposits, a clear unconformity (H1) is interpreted as the erosional surface formed following transgressive flooding of the basin sill. The Gulf of Corinth deviates from eustatic sea-level fluctuations due to a sill at its western entrance, currently at ~60–65 m depth (Perissoratis et al., 2000), with a lowstand lake level thought to be close to this depth. Away from major active faults, the shelf edge (a lowstand feature) is close to current sill depth, supporting the assumption that the sill has not changed depth significantly in the recent past. A consistent age range for H1 can be estimated from the depth of the basin sill, paleo-shelf elevation range, eustatic sea level curves and dated samples. The seaward-dipping transgressive surface rises from the shelf edge to a minimum of ~40–50 m close to the current coastline (allowing for the effects of Holocene fault displacement). Radiocarbon dates from cores within and outside the study area produce ages just above the horizon of ~9.5–12 ka BP (Perissoratis et al., 2000; Collier et al., 2000; Lemeille et al., 2004). Combining these data with eustatic sea level curves (e.g., Siddall et al., 2003) we estimate sill flooding at ~11–13 ka and flooding of the Aigion paleo-shelf and hence the unconformity (H1) age at ~10–13 ka.

Geometry of the Aigion and Offshore Aigion Fault Systems

The E-W trending Aigion fault system consists of multiple onshore segments (AF) and is thought to continue onto the shelf (OAF) to the east (Fig. 1; Koukouvelas and Doutsos,

1996; Koukouvelas, 1998; Palyvos et al., 2005; Soter and Katsonopoulou, 1998). Footwall topography and presumably total fault displacement on the main fault segment (AF) at Aigion town gradually decreases from west to east. The main fault probably terminates at or just west of the Meganitis river, but other authors continue the fault further west (Koukouvelas, 1998). West of the Meganitis river and towards the Phoenix River, Palyvos et al. (2005) interpret a series of NW-SE and E-W fault segments (Fassouleika and Selinitika, Fig. 1) along the range front and incorporate these into a larger complex Aigion-Neos-Erineos fault system (ANEFS). East of Aigion town, several authors have proposed an additional segment underlying the Selinous delta (Koukouvelas, 1998; Pantosti et al., 2004), but surface expression is minimal.

New seismic data confirm the activity of the eastern offshore part of this fault system and reveal its complex surface and sub-surface geometry (Fig. 3; Cotterill, 2006). The fault system (OAF, Fig. 1) consists of two main faults (1 and 2, Figures 2, 3) forming a graben, and a number of minor faults within the graben and footwalls (Fig. 3). Pockmarks are common and in places are distributed linearly indicating sub-surface blind faults. Three main segments of fault 1, west (A), central (B) and east (C), coincide with left steps in the fault geometry. A change in polarity of the northern fault (2), from S- to N-dipping, is coincident with a significant left step of the southern fault (1) and associated transfer zone with complex faulting between segments B and C. East of this location towards the shelf edge, the graben narrows and there is a significant drop in net displacement (Fig. 3). Other seismic profiles from this study indicate further displacement east of the shelf fault system, suggesting that the fault system damage zone continues a further ~1 km east of the shelf edge. Coastal field investigations along strike from the offshore OAF trace reveal small recent scarps down to the north (Fig. 3). These may be equivalent to the cumulative scarps identified by Pantosti et al. (2004) further west on the Selinous fan delta. In total, the OAF can therefore be traced for at

least ~3 km from the coast to just east of the shelf edge (Fig. 3). The N and S-dipping fault splays must converge at a depth of >0.5 km, assuming fault dips of 50–60°.

Aigion Area Faulting

North of the OAF, the E-W trending Cape Gyftisa fault (CGF, Fig. 1) displaces the seafloor and controls the shelf edge; the displacement and seafloor offset decreases westward toward Cape Gyftisa. Offset of the transgressive surface on several seismic profiles indicates a Holocene slip rate of 1.7 ± 0.5 mm/yr for the CGF. The minor fault in Aigion harbour (Fig. 1) is probably not active during the Holocene (from lack of deformation of youngest sediments) and is not clearly connected to the CGF. Figure 1 shows other significant offshore faults (this study; McNeill et al., 2005) with slip rates where estimated. No further major Holocene-active faults are recognized in the Aigion harbour area from our data, although mass wasting and 3D sedimentary-topographic architecture complicate the seismic interpretation.

Offshore Aigion Fault Slip Rate

Spatially averaged displacement of the transgressive horizon across fault 1 (Figs. 2 and 3) is 13 ± 3 m with a maximum of 22 m, and a total spatially averaged displacement across the entire system (all major and significant minor faults) of 27 ± 4 m and maximum of 35 m (1σ error, Figure 3; Cotterill, 2006). These displacements decrease close to the shelf edge at the eastern tip of the system at segment C (this segment was not included in displacement calculations). Using 10–13 ka for the transgressive horizon age, averaged Holocene displacement rates are $\sim 1.2 \pm 0.4$ mm/yr for fault 1 and $\sim 2.5 \pm 0.7$ mm/yr for the whole OAF fault system. No Holocene lateral fault propagation is measurable from our profile spacing.

DISCUSSION

Fault Slip Rates

Slip rates from several techniques and time periods for regional faults are summarized in Figure 1. To assess slip rates on the Aigion fault (AF), we could simply use the late Pleistocene footwall uplift rate of 1–1.2 mm/yr (DeMartini et al., 2004). Locally and globally derived uplift:subsidence ratios of ~1:2-3 (McNeill and Collier, 2004) then yield a slip rate of ~4–7 mm/yr. Dislocation modeling produces a maximum slip rate of 9-11 mm/yr (DeMartini et al., 2004). Alternatively, we can combine subsidence rates from lowstand deltaic clinoforms and shorelines 1–2 km due north of the Aigion fault and Aigion town (McNeill et al., 2005) with footwall terrace uplift rates; both locations are close to the western fault tip where displacements appear highest. Two end-lowstand shorelines are present at ~80–85 m and ~165 m depth. The latter appears to have subsided post-deposition due to slope failure or local faulting, but careful seismic interpretation suggests that the younger clinoform unit is in situ locally. Assuming an age of 11–13 ka, the youngest shoreline produces a subsidence rate of ~1.3–2.5 mm/yr (adjusted for distance from the Aigion fault, e.g., Armijo et al., 1996). The depth of the youngest shoreline contrasts with interpreted end lowstand coastal deposits at ~68 m in the AIG-10 borehole (Lemeille et al., 2004) which produce maximum subsidence rates of 0.7 mm/yr; the comparison is probably complicated by multiple fault splays of the Aigion system close to the borehole site. Combining the late Quaternary rates of uplift (1–1.2 mm/yr) with Holocene subsidence (~1–2.5 mm/yr) and a fault dip of 60° we calculate slip rates of ~2.5–4.5 mm/yr. We note that this slip rate may combine multiple fault splays and that it combines Holocene subsidence with late Quaternary uplift, therefore representing an averaged rate over this time period. This is in good agreement with maximum late Holocene paleoseismological rates for this fault (Pantosti et al., 2004) and a little lower than late Quaternary rates from applying an uplift:subsidence ratio for this and other Corinth faults (4–7 mm/yr).

Fault Age

The age of the Aigion fault system can be estimated from the maximum age of uplifted marine terraces or by combining total offset with slip rate. Previous studies have produced conflicting estimates of the age of the AF ranging from 300 to 25 ka. Naville et al. (2004) and Cornet et al. (2004) used seismic refraction data and vertical seismic profiles around the AIG-10 borehole (0.5 km north of Aigion town and the AF) to suggest total basement offset of only ~150 m. Applying a post-~35 ka slip rate of 3.5 mm/yr to uplifted and subsided dated deposits (Lemeille et al., 2002; 2004) to this offset yields a young fault age of ~50 ka (Cornet et al., 2004). A similar age of 25–70 ka (Micarelli et al., 2003) was suggested by interpreting the Aigion town topographic scarp height (150 m) as total offset and applying a similar slip rate of 2–5 mm/yr. However, we support the older age estimate (200–300 ka) from the correlated and partially dated uplifted footwall terraces of DeMartini et al. (2004), based on the following arguments. The Aigion fault footwall uplift from the elevation of marine terraces (~230 m, DeMartini et al., 2004) alone equals or exceeds the borehole fault displacement requiring no hangingwall subsidence for consistency. The number and elevation of mapped footwall terraces are inconsistent with an age of ~50 ka and yield good correlation with Oxygen Isotope Stage 5 and 7 highstands. In addition, we question the use of topographic elevation of a cumulative fault scarp (not total footwall uplift) as total fault displacement and therefore the fault age of Micarelli et al. (2003). The lack of evidence of Holocene lateral fault growth from this study would also be unusual for a fault age of only 25–70 ka. These results support the view that the borehole stratigraphy or topographic scarp elevation should not be used to determine fault age. These problems were noted by Lemeille et al. (2004), who argued that additional fault splays may affect borehole stratigraphy.

Length and Displacement Profile of the Aigion Fault System

Based on their similar trends, locations and slip rates, we infer that the AF at Aigion town and the coastal and shelf segments (OAF) represent parts of a single system. No clear

175 fault trace is visible between the AF and OAF, although Pantosti et al. (2004) identified a 1 m
176 cumulative scarp coincident with cracks from the 1995 earthquake. The displacement profile
177 of the OAF also implies that the fault continues westward onto the delta (Fig. 3). We support
178 Pantosti et al.'s (2004) view that topographic fault expression is suppressed by burial/erosion
179 of the actively growing delta. Combining the offshore segment of the Aigion fault (OAF) with
180 confirmed onshore Aigion fault traces produces a total fault length of ≥ 10 km (Meganitis
181 River to east of the shelf edge, Fig. 1) similar to other major fault lengths (10–20 km) in the
182 Gulf. This combined fault system also produces a similar length and position to the
183 overlapping WEF to the south (Fig. 1). We conclude that the Aigion to offshore Aigion fault
184 system are one structure whereas the series of shorter fault segments to the northwest
185 (Palyvos et al., 2005) represent a separate fault system.

186 The slip rate of 2.5 ± 0.7 mm/yr on the offshore Aigion fault (OAF) is less than that of
187 the main Aigion fault but is within error. If displacement decreases linearly to zero at the tip,
188 the eastern fault tip must lie significantly east of the shelf edge; more likely the fault
189 displacement profile is non linear and fairly rapidly decreases to zero close to the shelf edge,
190 as for more mature Corinth fault systems (e.g., McNeill and Collier, 2004). No further
191 offshore trace of the fault is identified east of that shown in Figure 3 and displacement rates
192 and Holocene sediment thicknesses along the eastern OAF reveal a rapid decrease in slip
193 toward the shelf edge and increased geometric complexity (Fig. 3), all supporting the latter
194 hypothesis. The complex geometry of the offshore fault system is reminiscent of a fault tip
195 damage zone also supporting this as the tip location of the overall fault system.

196 SUMMARY

197 Broadly consistent uplift rates for the last 200–300 k.y. across the western parts of the
198 AF and WEF footwalls (DeMartini et al., 2004) suggest rapid transfer of strain from this
199 section of the southern to northern fault, either before OIS 9 or between OIS 9 and 7. Uplift of

the eastern AF-OAF footwall and subsidence of the eastern WEF hangingwall appears balanced with no net Holocene movement of the intervening delta plain (Soter, 1998). This supports division of the WEF into two segments east and west of the Selinous River, with the different behavior of the two segments presumably part of the process of shifting extension from an established fault (WEF) to a young fault (AF-OAF) in its hangingwall. The Aigion Fault system is similarly divided into two parts: (1) the main Aigion fault system (AF) and (2) the coastal plain fault segment and the OAF. The absence of measurable Holocene lateral propagation toward the eastern fault tip may indicate that this fault system with slip rate up to ~5 mm/yr has completed its lateral growth rapidly within 200–300 ka. This supports Walsh et al.'s (2002) proposal that faults develop and grow to their maximum length rapidly, but contrasts with studies indicating slower development (e.g., Taylor et al., 2004). Rapid growth and fault development is supported by the transfer of strain between the western parts of the WEF and AF/OAF fault systems and absence of lateral propagation at the eastern tip in the last ~10 k.y.. The displacement profile of the offshore part of the fault toward the coast supports a fault segment in the active delta area linking the offshore fault to the main Aigion fault segment and a total fault length of ~10 km. The maximum slip rate is compatible with other Gulf faults but when all regional faults are summed, leads to high extensional strain across this part of the rift. The geometric complexity and number of basement-offsetting faults (those with slip rate of >1–2 mm/yr) across the rift at this location is unusual and may be the result of changes in basement properties or crustal thickness.

ACKNOWLEDGMENTS

We thank the crew of the *MV Vassilios G* for their expertise during the survey and technical and scientific contributions from Richard Collier, Mike Leeder, George Ferentinos, George Papatheoderou, Chris Malzone, John Davis, and Aggeliki Georgiopolou. The Greek authorities are thanked for permission to conduct this work. We

thank F. Cornet, D. Pantosti and an anonymous reviewer for their thorough reviews.

Research was funded by NERC grant NER/B/S/2001/00269, University of Southampton,
the Royal Society and JREI (HEFCE/HEFCW).

REFERENCES CITED

- Armijo, R., Meyer, B., King, G.C.P., Rigo, A., and Papanastassiou, D., 1996, Quaternary evolution of the Corinth Rift and its implications for the Late Cenozoic evolution of the Aegean: *Geophysical Journal International*, v. 126, p. 11–53.
- Collier, R.E.L., Leeder, M.R., Trout, M., Ferentinos, G., Lyberis, E., and Papatheodorou, G., 2000, High sedimentary yields and cool, wet winters: Test of last glacial paleoclimates in the northern Mediterranean: *Geology*, v. 28, p. 999–1002, doi: 10.1130/0091-7613(2000)028<0999:HSYACW>2.3.CO;2.
- Cornet, F.H., Doan, M.L., Moretti, I., and Borm, G., 2004, Drilling through the Aigion fault: the AIG10 well observatory: *Comptes Rendus Geoscience*, v. 336, p. 395–406, doi: 10.1016/j.crte.2004.02.002.
- Cotterill, C.J., 2006, A high-resolution Holocene fault activity history of the Aigion shelf, Gulf of Corinth, Greece: PhD thesis, University of Southampton.
- DeMartini, P.M., Pantosti, D., Palyvos, N., Lemeille, F., McNeill, L., and Collier, R., 2004, Slip rates of the Aigion and Eliki faults from uplifted marine terraces, Corinth Gulf, Greece: *Comptes Rendus Geoscience*, v. 336, p. 325–334, doi: 10.1016/j.crte.2003.12.006.
- Koukouvelas, I.K., 1998, The Eigion fault, earthquake-related and longterm deformation, Gulf of Corinth, Greece: *Journal of Geodynamics*, v. 26, p. 501–513, doi: 10.1016/S0264-3707(97)00046-X.

- 248 Koukouvelas, I.K., and Doutsos, T., 1996, Implications of structural segmentation during
249 earthquakes: the 1995 Egion earthquake, Gulf of Corinth, Greece: *Journal of Structural*
250 *Geology*, v. 18, p. 1381–1388, doi: 10.1016/S0191-8141(96)00071-5.
- 251 Leeder, M.R., Portman, C., Andrews, J.E., Collier, R.E.L., Finch, E., Gawthorpe, R.L.,
252 McNeill, L.C., Perez-Arlucea, M., and Rowe, P., 2005, Normal faulting and crustal
253 deformation: Alkyonides Gulf and Perachora peninsula, eastern Gulf of Corinth rift basin,
254 Greece: *Journal Geological Society of London*, 162, 549-561.
- 255 Lemeille, F., Sorel, D., Bourdillon, C., Guernet, C., Manakou, M., and Berge-Thierry, C.,
256 2002, Quantification of the deformation associated with the active Aigion fault (Gulf of
257 Corinth, Greece) using the study of Upper Pleistocene and Holocene marine
258 transgression deposits: *Comptes Rendus Geoscience*, v. 334, p. 497–504, doi:
259 10.1016/S1631-0713(02)01781-9.
- 260 Lemeille, F., Chatoupis, F., Fouvelis, M., Rettenmaier, D., Unkel, I., Micarelli, L., Moretti,
261 I., Bourdillon, C., Guremet, C., and Muller, C., 2004, Recent syn-rift deposits in the
262 hangingwall of the Aigion fault (Gulf of Corinth, Greece): *Comptes Rendus Geoscience*,
263 336, 425–434.
- 264 McNeill, L.C., and Collier, R.E., LL., 2004, Footwall uplift rates of the Eastern Eliki Fault,
265 Gulf of Corinth, Greece, inferred from Holocene and Pleistocene terraces: *Journal*
266 *Geological Society of London*, v. 161, p. 81–92.
- 267 McNeill, L., Cotterill, C., Stefatos, A., Henstock, T., Bull, J., Collier, R., Papatheoderou, G.,
268 Ferentinos, G., and Hicks, S., 2005, Active faulting within the offshore western Gulf of
269 Corinth, Greece: implications for models of continental rift deformation: *Geology*, v. 33,
270 p. 241–244, doi: 10.1130/G21127.1.

- 271 Micarelli, L., Moretti, I., and Daniel, J.-M., 2003, Structural properties of rift-related normal
272 faults: case study in the Gulf of Corinth, Greece: *Journal of Geodynamics*, v. 36, p. 275–
273 303, doi: 10.1016/S0264-3707(03)00051-6.
- 274 Moretti, I., Sakellariou, D., Lykousis, V., and Micarelli, L., 2003, The Gulf of Corinth: An
275 active half graben?: *Journal of Geodynamics*, v. 36, p. 323–340, doi: 10.1016/S0264-
276 3707(03)00053-X.
- 277 Naville, C., Serbutoviez, S., Moretti, I., Daniel, J.-M., Throo, A., Girard, F., Sotiriou, A.,
278 Tselentis, A., Skarpezelos, C., Brunet, C., and Cornet, F.H., 2004, Pre-drill surface seismic
279 in the vicinity of the AIG-10 well and post-drill VSP: *Comptes Rendus Geoscience*, 336,
280 407–414.
- 281 Palyvos, N., Pantosti, D., De Martini, P.M., Lemeille, F., Sorel, D., and Pavlopoulos, K.,
282 2005, The Aigion-Neos Erineos coastal normal fault system (Western Corinth Gulf rift,
283 Greece): geomorphological signature, recent earthquake history and evolution: *Journal of*
284 *Geophysical Research*, v. 110, doi: 10.1029/2004JB003165, doi: 10.1029/2004JB003165.
- 285 Pantosti, D., DeMartini, P.M., Koukouvelas, I., Stamatopoulos, L., Palyvos, N., Pucci, S.,
286 Lemeille, F., and Pavlides, S., 2004, Paleoseismological investigations of the Aigion fault
287 (Gulf of Corinth, Greece): *Comptes Rendus Geoscience*, v. 336, p. 335–342, doi:
288 10.1016/j.crte.2003.12.005.
- 289 Perissoratis, C., Piper, D.J.W., and Lykousis, V., 2000, Alternating marine and lacustrine
290 sedimentation during late Quaternary in the Gulf of Corinth rift basin, central Greece:
291 *Marine Geology*, v. 167, p. 391–411, doi: 10.1016/S0025-3227(00)00038-4.
- 292 Rigo, A., Lyon-Caen, H., Armijo, R., Deschamps, A., Hatzfeld, D., Makropoulos, K.,
293 Papadimitriou, P., and Kassaras, I., 1996, A microseismic study in the western part of the
294 Gulf of Corinth (Greece): implications for large-scale normal faulting mechanisms.
295 *Geophysical Journal International*, v.126, 663–688.

- Siddall, M., Rohling, E.J., Almogi-Labin, A., Hemleben, C., Meischner, D., Schmelzer, I.,
and Smeed, D., 2003, Sea-level fluctuations during the last glacial cycle: *Nature*, v. 423,
p. 853–858, doi: 10.1038/nature01690.
- Soter, S., 1998, Holocene uplift and subsidence of the Helike Delta, Gulf of Corinth, Greece:
in Stewart, I.S., and Vita-Finzi, C. (eds.), *Coastal Tectonics*. Geol. Soc. London Spec.
Pub., 146, p. 41–56.
- Soter, S., and Katsonopoulou, D., 1998, The search for ancient Helike 1988–1995:
geological, sonar, and borehole studies: in Katsonopoulou, D., Soter, S., and Schilardi, D.
(eds.), *Ancient Helike and Aigialeia: Proceedings of the Second International
Conference*, Helike Society, Athens.
- Stefatos, A., Papatheoderou, G., Ferentinis, G., Leeder, M., and Collier, R., 2002, Active
offshore faults in the Gulf of Corinth, Greece: Their seismotectonic significance: *Basin
Research*, v. 14, p. 487–502, doi: 10.1046/j.1365-2117.2002.00176.x.
- Stewart, I., 1996, Holocene uplift and palaeoseismicity on the Eliki fault, Western Gulf of
Corinth, Greece: *Annali di Geofisica*, v. 39, p. 575–588.
- Taylor, S.K., Bull, J.M., Lamarche, G., and Barnes, P.M., 2004, Normal fault growth and
linkage during the last 1.3 million years: an example from the Whakatane Graben, New
Zealand: *Journal of Geophysical Research*, v. 109, p. B02408, doi:
10.1029/2003JB002412, doi: 10.1029/2003JB002412.
- Walsh, J.J., Nicol, A., and Childs, C., 2002, An alternative model for the growth of faults:
Journal of Structural Geology, v. 24, p. 1669–1675, doi: 10.1016/S0191-8141(01)00165-
1.

FIGURE CAPTIONS

Figure 1. Geometry of Aigion fault system, other onshore and major offshore faults with slip
rates (sources: 1-This study; 2-McNeill and Collier, 2004; 3-Stewart, 1996; DeMartini et al.,

2004; 5-McNeill et al., 2005; 6-Pantosti et al., 2004; 7-Palyvos et al., 2004). Bold indicates slip rates from offset horizons across faults, others estimated from uplift or subsidence only. Underlined rates are short-term (Holocene), non-underlined are long-term (late Quaternary). Rates from paleoseismology (6, 7) may be minima. Offshore faults from this study, McNeill et al. (2005) and Stefatos et al. (2002). Dotted line = range front; shaded areas = marine terraces. Inset 1 regional map. Inset 2 of boomer seismic tracklines over offshore Aigion fault (OAF), with location of seismic profile in Figure 2 in bold. Faults: AF—Aigion; OAF—Offshore Aigion; CGF—Cape Gyftisa; FF—Fassouleika; SF—Selinitika; NEF—N Eratini; SEF—S Eratini; SCF—Sub-Channel; WEF—W Eliki; EEF—E Eliki; CG—Cape Gyftisa; Star—Aigion town.

Figure 2. Prestack depth-migrated boomer seismic profile (Figure 1 for location) across the Offshore Aigion fault system (OAF). Faults 1 and 2 bound the main offshore graben. Distribution of other faults shown in Figure 3. Vertical exaggeration = 6–7 at seafloor. H1 is transgressive flooding surface (10–13 ka) separating late Quaternary lacustrine and subaerial deposits from Holocene marine deposits.

Figure 3. (A) Multibeam bathymetry of Offshore Aigion fault system (1.5 m grid) and Holocene active fault interpretation (surface breaking faults solid, subsurface/blind (within 50 m of surface) faults dashed). Main faults (blue) labeled 1 and 2, major surface segments A, B, C of fault 1. Photo shows possible recent scarp at coast (~38.25°N, 22.13°E). (B) E-W-aligned displacement profile of net OAF system and fault 1 at horizontal scale of map.

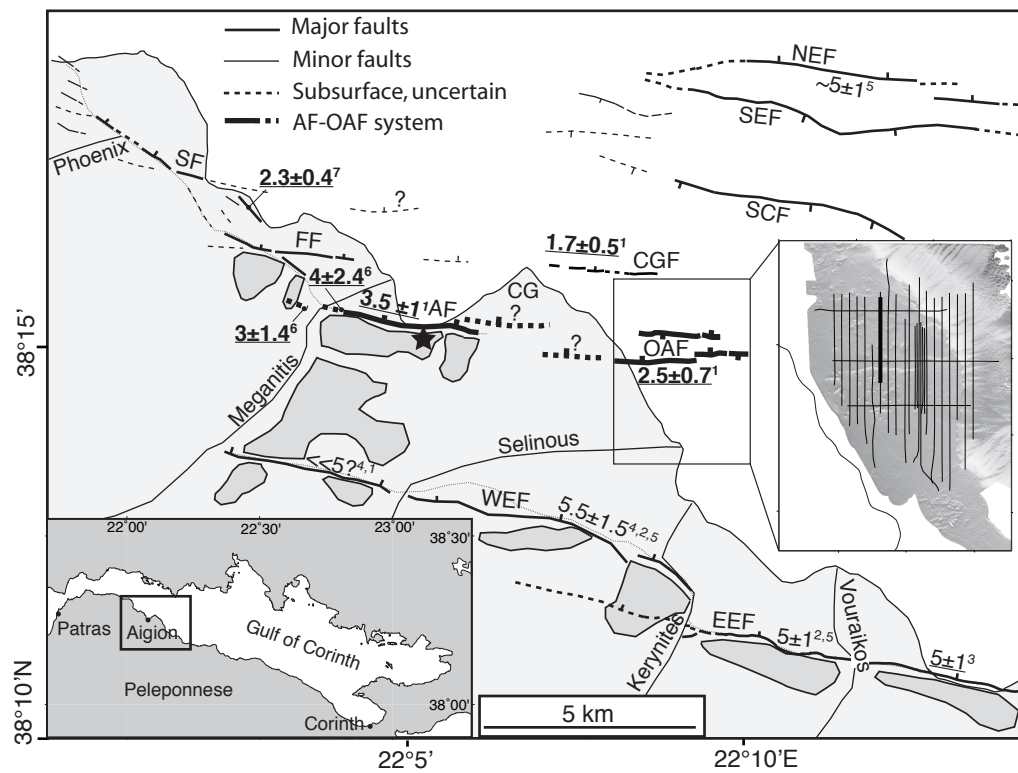


Figure 1, McNeill et al.

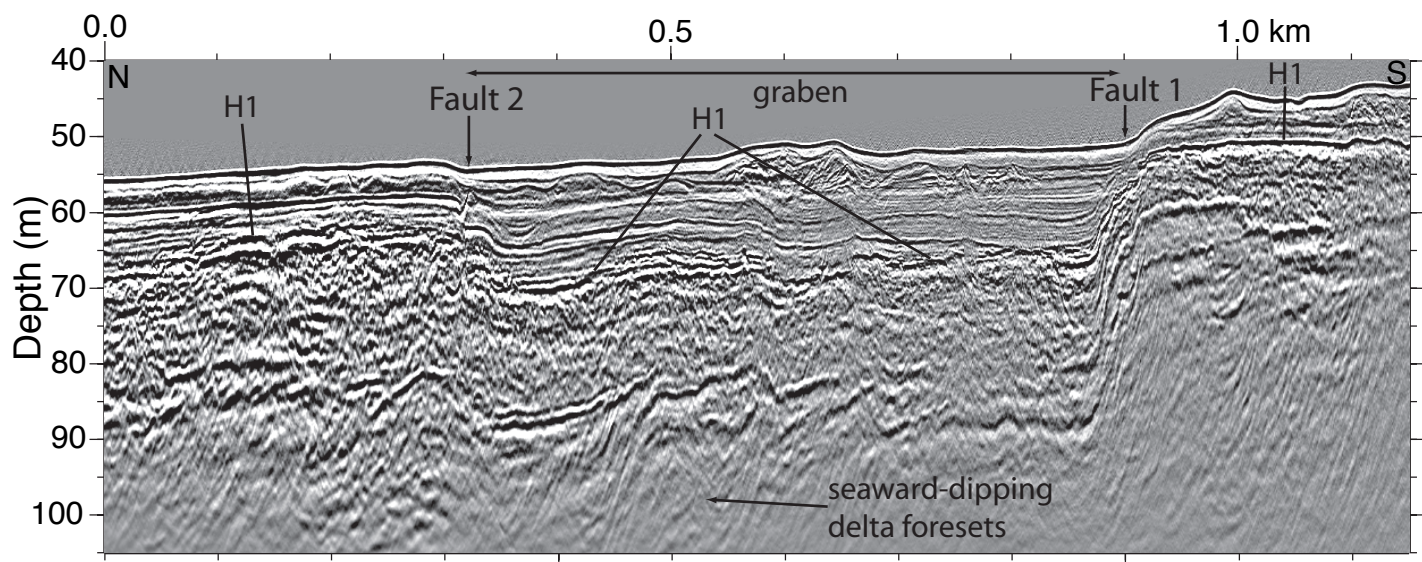


Figure 2, McNeill et al.

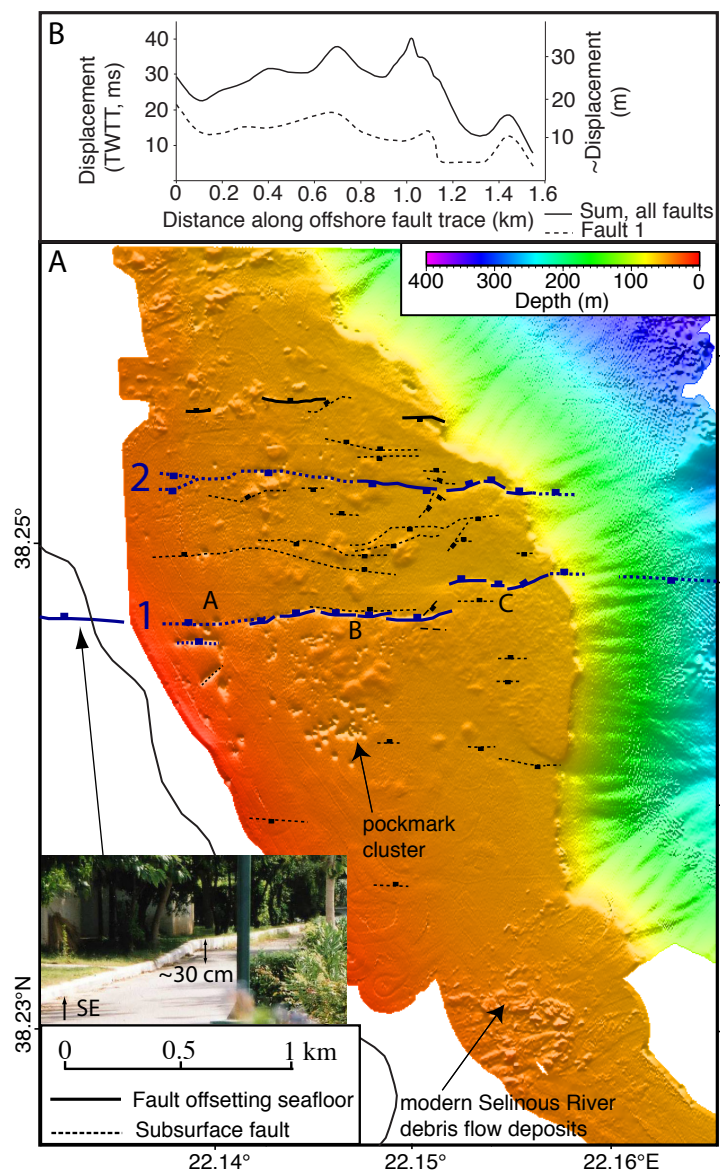


Figure 3, McNeill et al.